Stark-induced adiabatic Raman passage for preparing polarized molecules

Nandini Mukherjee and Richard N. Zare[a)]
Department of Chemistry, Stanford University, Stanford, California 94305-5080, USA

(Received 7 February 2011; accepted 19 May 2011; published online 8 July 2011)

We propose a method based on Stark-induced adiabatic Raman passage (SARP) for preparing vibrationally excited molecules with known orientation and alignment for future dynamical stereochemistry studies. This method utilizes the (J, M)-state dependent dynamic Stark shifts of rovibrational levels induced by delayed but overlapping pump and Stokes pulses of unequal intensities. Under collision-free conditions, our calculations show that we can achieve complete population transfer to an excited vibrational level ($v > 0$) of the H_2 molecule in its ground electronic state. Specifically, the H_2 ($v = 1,\ J = 2,\ M = 0$) level can be prepared with complete population transfer from the ($v = 0,\ J = 0,\ M = 0$) level using the S(0) branch of the Raman transition with visible pump and Stoke laser pulses, each polarized parallel to the $\hat{z}$ axis (uniaxial $\pi - \pi$ Raman pumping). Similarly, H_2 ($v = 1,\ J = 2,\ M = \pm 2$) can be prepared using SARP with a left circularly polarized pump and a right circularly (or vice versa) polarized Stokes wave propagating along the $\hat{z}$ axis ($\sigma^{\pm} - \sigma^{\mp}$ Raman pumping). This technique requires phase coherent nanosecond pulses with unequal intensity between the pump and the Stokes pulses, one being four or more times greater than the other. A peak intensity of $\sim$16 GW/cm^2 for the stronger pulse is required to generate the desirable sweep of the Raman resonance frequency. These conditions may be fulfilled using red and green laser pulses with the duration of a few nanoseconds and optical energies of $\sim$12 and 60 mJ within a focused beam of diameter $\sim$0.25 mm. Additionally, complete population transfer to the $v = 4$ vibrational level is predicted to be possible using SARP with a 355-nm pump and a near infrared Stokes laser with accessible pulse energies. © *2011 American Institute of Physics*. [doi:10.1063/1.3599711]

I. INTRODUCTION

To study dynamical stereochemistry, researchers need to prepare polarized molecular targets in the excited states of a given vibrational level within the ground electronic surface.[1–7] For the alignment and orientation of polar molecules in excited ($v = 2$, J) rovibrational levels, we previously proposed a method[8,9] using infrared stimulated Raman adiabatic passage (IR STIRAP). For this method, the alignment and orientation refer to polarization of the quantum mechanical angular momentum vector $\boldsymbol{J}$. An aligned molecular sample has the direction of its $\boldsymbol{J}$ so that the $|M|$ values of its projection on some quantization axis are unequally populated; an oriented molecular sample has unequal populations in $+M$ and $-M$ sublevels.

In this paper, we consider the alignment and orientation of nonpolar molecules (for example, H_2) in excited rovibrational levels using nanosecond visible laser pulses. In the absence of a real intermediate level, one expects a substantial population transfer when the Raman resonance condition $\omega_{10} = \omega_P - \omega_S$ is satisfied, where ω_{10} is the resonance frequency for the $v = 0 \rightarrow v = 1$ vibrational transition within the ground electronic surface and ω_P and ω_S are the optical frequencies for the pump and Stokes laser beams, respectively.[10–13] However, in reality, in a collision-free ambience, such as in a supersonic molecular beam, up to 50% population can only be transferred to the excited vibrational level at saturation using either coherent or incoherent (broad-band) pump and Stokes laser pulses with intensities in the range of $\sim$10 GW/cm^2.

We present a technique based on Stark-induced adiabatic Raman passage (SARP) that transfers an entire population to a desired rovibrational (v, J, M) eigenstate. Molecular polarizability and dynamic (AC) Stark shifts depend on the molecular orientation (M-dependence), which is relative to the polarization direction of the laser's optical field. To achieve complete population transfer, SARP exploits the M-dependent dynamic Stark shifts of the rovibrational (v, J) levels with a delayed sequence of overlapping pump and Stokes pulses of unequal intensities. The central idea is to drive an adiabatic passage process by sweeping the Raman transition frequency across the two-photon resonance. Grischkowski, Loy, and Liao[14–17] first introduced the idea of chirped adiabatic passage for a two-photon transition utilizing the dynamic Stark shifts of the resonant levels. In their example, the relative Stark shift of the two-photon resonant levels was enhanced by tuning closer to a single-photon intermediate level. However, for Raman excitation of H_2, an intermediate level in the visible or near UV does not exist to enhance the relative Stark shift of the resonant vibrational levels. In the absence of an intermediate level, the visible pump and Stokes lasers shift the vibrational levels of the ground electronic state in a similar way if we ignore the orientational dependence, thus cancelling the net Stark shift of the ($v = 0 \rightarrow v = 1$) Raman transition. In this situation, SARP might be thought to be unachievable. By accounting for the M-dependent

a)Author to whom correspondence should be addressed. Electronic mail: zare@stanford.edu.

polarizability, our calculations show that there is an appreciable dynamic Stark shift of the resonance frequency which attains a maximum for an *S*-branch Raman transition. The *M*-dependent dynamic Stark shifts in stimulated Raman pumping have been utilized earlier by Rudert *et al.*[18] to spatially orient molecules in the excited rovibrational levels. They showed that different /*M*/ substates of the vibrationally excited acetylene molecule can be selected (thus aligning ***J***) using different polarizations of the pump and Stokes laser pulses of duration 8 ns and peak intensities >100 GW/cm^2.

Complete population inversion between vibrational levels of the electronic ground state of molecules via a resonant intermediate level in the excited electronic state has been demonstrated previously using STIRAP by Bergmann and co-workers.[19–21] STIRAP, however, degrades when the two-photon resonance condition is perturbed by the dynamic Stark shifts (especially of the excited electronic state) which may be unavoidable at the optical intensity required by the Raman adiabatic passage. To solve this problem, Bergmann and co-workers introduced Stark chirped rapid adiabatic passage (SCRAP) which was first applied to invert populations in a two-level 2*s*-3*s* He transition[22,23] using an additional Stark pulse that swept the frequency of the 2*s*-3*s* transition. For the purpose of inverting population among the vibrational levels of an electronic ground state, SCRAP was later generalized to a three-level up-down pumping configuration (Λ system) with a real intermediate level as an excited electronic state.[24] In this case the single photon pump and Stokes transitions of the Λ system were swept through their respective resonances using an additional Stark pulse that preferentially shifted the intermediate level. Using this method, also known as double SCRAP or D-SCRAP, population inversion between the vibrational levels of nitric oxide was achieved via two successive adiabatic passages one for each arm of the Λ system. For many molecules (such as H_2), tuning to the pump and Stokes transitions of a Λ system connecting the vibrational levels of the ground electronic state to an intermediate excited electronic state will require tunable vacuum ultraviolet laser pulses, which can be challenging experimentally.

SARP takes advantage of the *M*-dependent Stark shifts of the rovibrational levels and builds along the line of previous works on Stark induced adiabatic passage of Grischkowski's and Bergmann's groups. The advantage of SARP, however, is that it accomplishes population inversion in molecules such as H_2 utilizing more accessible visible and standard UV laser sources where a real intermediate level is not required. This means that the single photon detuning Δ associated with the pump and Stokes transitions far exceeds the Raman resonance frequency $\omega_{v_0 v}$ (i.e., $\Delta \gg \omega_{v_0 v}$) between the vibrational levels v_0 and v. Moreover, SARP does not require an additional Stark pulse for chirping the Raman resonance frequency; the Raman frequency is swept through resonance by the time-varying intensity of the temporally shifted but overlapping pump and Stokes pulses.

We note that to invert population among the vibrational levels of a molecule with widely separated electronic levels such as in H_2 or N_2, SCRAP will require near resonant multiphoton pump and multiphoton Stokes transitions as suggested in Ref. 24. The high optical intensity that is required for the process will also enhance the probability of resonant multiphoton ionization and dissociation of the real intermediate level in the excited electronic state. SARP has been designed to avoid the photofragmentation associated with a real intermediate state as in D-SCRAP.

Selective vibrational excitation in the absence of intermediate resonance can be also accomplished using chirped adiabatic Raman passage (CARP) proposed by Chelkowski *et al.*[25–27] As opposed to sweeping the molecular energy levels, CARP utilizes frequency swept (chirped) picosecond laser pulses which requires high peak intensity $\sim >1000$ GW/cm^2 to fulfill the condition of adiabatic passage. Note that SARP avoids the technical challenge of sweeping the carrier frequency of nanosecond pulses using electro-optical method that requires appropriately shaped voltage pulses (several kV/mm) over nanoseconds to produce adequate phase modulation.

The theoretical framework for SARP is built around the $v = 0$ to $v = 1$ transition but the analysis remains applicable to allowed Raman transitions between any pair of vibrational levels of polar and nonpolar molecules. Our theoretical analysis is extended to $\Delta v = 4$ showing that the larger *M*-dependent polarizabilities and Stark shifts of the higher vibrational levels works in favor of SARP so that population inversion can be attained using standard laser sources with reasonable optical energies.

The paper is organized as follows: In Sec. II we elaborate the coherent dynamics of stimulated Raman pumping using the density matrix formalism and introduce SARP using the optical Block equations (a two-photon vector model). In Sec. III we present the results of numerical calculations showing the feasibility of exciting the $v = 1$ level of the H_2 molecule using the temporally displaced visible pump and Stokes laser pulses of nanosecond duration. We also describe the practical implementation of SARP using optical sources necessary to carry out the adiabatic passage. In Sec. IV we discuss how SARP can achieve complete population transfer in the H_2 $v = 0 \rightarrow v = 4$ transition using standard UV and near infrared laser sources. In Sec. V we briefly summarize our conclusions.

II. POPULATION TRANSFER USING SARP

In the absence of an intermediate resonance, the stimulated Raman transition $v = 0 \rightarrow v = 1$ driven by the coherent pump and Stokes fields is reduced to the problem of a two-photon resonant two-level system. Using a graphical method,[28] we derived the density matrix equations describing the two-photon Raman transition in the presence of $\hat{z}$ polarized pump and Stokes optical fields $\vec{E}_P = E_P \hat{z} e^{i\omega_P t} + c.c.$, and $\vec{E}_S = E_S \hat{z} e^{i\omega_S t} + c.c.$ Our derivation utilizes the "adiabatic following approximation" to eliminate the off-resonant density matrix elements as described in detail in Ref. 28. The expressions for the two-photon Rabi frequency and dynamic Stark shifts are generated automatically from the diagrammatic expansion of the density matrix. Significant theoretical work has been done in the past for describing the multiphoton excitation in a multilevel atomic and molecular system.[29] Particularly relevant is the work of Chelkowski

et al.[25] who specifically addressed Raman pumping in the presence of large single photon detuning ($\Delta \gg \omega_{v_0 v}$) of the pump and Stokes transitions and presented derivations of the equations for the state amplitudes in the Schrödinger picture. Our graphical derivation agrees with that of Chelkowski *et al.*'s work. The density matrix equations are

$$\frac{d\sigma_{01}}{dt} + i\delta_2\sigma_{01} = i2rw, \tag{1}$$

$$\frac{dw}{dt} = -2\mathrm{Im}[r^*\sigma_{01}]. \tag{2}$$

Here, σ_{01} is the two-photon Raman coherence between the $v = 0$ and $v = 1$ vibrational levels. $w = (\rho_{11} - \rho_{00})/2$ where, ρ_{11} and ρ_{00} are the populations in $v = 1$ and $v = 0$ levels, respectively. The populations are normalized so that $\rho_{00} + \rho_{11} = 1$. The two-photon generalized Rabi frequency r is

$$r = \frac{E_P E_S^*}{\hbar^2}\sum_k \mu_{0k}\mu_{k1}\left[\frac{1}{(\omega_{k0} - \omega_P)} + \frac{1}{(\omega_{k0} + \omega_S)}\right], \tag{3}$$

where E_P and E_S are the time-dependent optical field amplitudes associated with the pump (at frequency ω_P) and Stokes (at frequency ω_S) laser pulses, respectively. μ_{ik} and $\omega_{ki}(= \omega_{v'v})$ are the transition dipole moments and the resonance frequency between the ith ($i \equiv v = 0, 1$) and kth vibronic levels (v') belonging to the ground and excited electronic states, respectively. The net time-dependent detuning δ_2 for $v = 0 \rightarrow v = 1$ Raman transition is given by

$$\begin{aligned}\delta_2 &= (\omega_P - \omega_S - \omega_{10}) - \delta_{AC} - i\gamma \\ &= \delta_0 - i\gamma - \left(\delta_1^{AC} - \delta_0^{AC}\right).\end{aligned} \tag{4}$$

Here, γ is the phase damping rate for the Raman coherence σ_{01} in presence of collisions. δ_{AC} is the time-dependent dynamic Stark shift of the Raman transition frequency in presence of intense nanosecond pulses. $\delta_0 = \omega_P - \omega_S - \omega_{10}$ is the zero-field detuning of the Raman transition. δ_1^{AC} and δ_0^{AC} are the dynamic Stark shifts of the vibrational levels $v = 0$ and $v = 1$, respectively. Specifically, for the level $i = 0,1$

$$\delta_i^{AC} = -\frac{1}{\hbar}[\alpha_i(\omega_P)|E_P|^2 + \alpha_i(\omega_S)|E_S|^2], \tag{5}$$

where, $\alpha_i(\omega_j)$ is the polarizability of the ith vibrational level

$$\alpha_i(\omega_j) = \frac{1}{\hbar}\sum_k |\mu_{ik}|^2\left[\frac{1}{(\omega_{ki} - \omega_j)} + \frac{1}{(\omega_{ki} + \omega_j)}\right], \tag{6}$$

and $i \equiv v = 0, 1$ and $\omega_j \equiv \omega_P$ or ω_S.

In Eqs. (1)–(6), all frequencies and rates of transitions are expressed in rad/s. It is important to include the M-dependence of the molecular polarization because it makes the dominant contribution to the unequal Stark shifts for the two rovibrational levels ($v = 0, v = 1$). To carry out the adiabatic passage we modulate the nonzero Stark shift δ_{AC} to sweep the net Raman detuning δ_2 by suitable choice of pulse intensities, shape, and delay.

A. The Bloch vector model for SARP

In the absence of phase damping ($\gamma = 0$), Eqs. (1) and (2) describe the rotation of a pseudo-vector (often called the two-photon Bloch vector) $\vec{R}$ around an angular velocity vector $\vec{F}$ (also referred to as the field vector) in a three-dimensional abstract space,[14–17,30–32]

$$\frac{d\vec{R}}{dt} = \vec{F} \times \vec{R}, \tag{7}$$

where $\vec{F} = \{-2r, 0, -\delta_2\}$ and $\vec{R} = \{\mathrm{Re}(\sigma_{01}), \mathrm{Im}(\sigma_{01}), w\}$. Besides resembling the Bloch equation for a nuclear spin in nuclear magnetic resonance, the rotation of the Bloch vector in Eq. (7) accurately describes the Raman excitation process as a function of time; the population transfer is given by $R_3 = w$ and the induced Raman coherence or polarization is described by R_2, $R_1 \propto \sigma_{01}$.

How does the Bloch vector rotate in the pseudo space under the action of the pump and Stokes laser pulses? At the starting point of the Raman interaction, we have $r \approx 0$, $\sigma_{01} \approx 0$, and $w \approx -0.5$. At this time, if the Raman detuning is $\delta_2 \neq 0$, both pseudo vectors $\vec{F}$ and $\vec{R}$ point parallel to the $\hat{z}$ axis of the abstract space. As the two-photon Rabi frequency r develops and the Raman detuning δ_2 is Stark-shifted under the action of the pump and Stokes laser pulses [see Eqs. (3)–(6)], the pseudo angular velocity vector $\vec{F}$ starts changing direction in the abstract space. If $\vec{F}$ changes sufficiently slowly compared to the angular velocity $|\vec{F}|$ with which $\vec{R}$ precesses around $\vec{F}$ then $\vec{R}$ will be able to keep up with the change and follow $\vec{F}$ adiabatically, tracing a narrow conical surface around it (staying almost parallel to $\vec{F}$) (Refs. 14–16 and 30–32) as shown in Fig. 1. The adiabatic following condition can be expressed mathematically as

$$\frac{|\Delta\vec{F}|}{|\vec{F}|} \propto \left|\frac{d\vec{F}}{dt}\right| \times \frac{1}{|\vec{F}|^2} < 1. \tag{8}$$

Equation (8) expresses the condition that the magnitude of the fractional change in $\vec{F}$ in a Rabi oscillation period, which is given by $1/|\vec{F}|$, is less than unity. Actually, this condition is rather forgiving and the adiabatic following does not require this quantity to be much less than unity. Equation (8) is similar to Eq. (8) in Ref. 14.

When the Raman detuning, δ_2 , sweeps from a negative to a positive value, or vice versa, during the two-photon interaction, the component of $\vec{F}$ along the $\hat{z}$ axis ($F_3 = -\delta_2$) reverses. In the presence of sufficient two-photon coupling field r the Bloch vector $\vec{R}$ stays locked and reverses direction simultaneously with $\vec{F}$ as shown in Fig. 1. Reversal of $\vec{R}$ implies a sign change of w with the result of complete population transfer to the $v = 1$ level.

How is δ_2 swept using a sequence of pump and Stokes pulses? For the visible pump and Stokes waves with far off-resonant electronic excited states (as in H_2 molecules), we may assume that $\alpha_i(\omega_P) \cong \alpha_i(\omega_S)$ for both vibrational levels ($i = 0, 1$). In this case, the net Stark shift δ_{AC} of the Raman resonance depends upon the difference in polarizabilities of the two vibrational levels. Following Eq. (5) the Raman

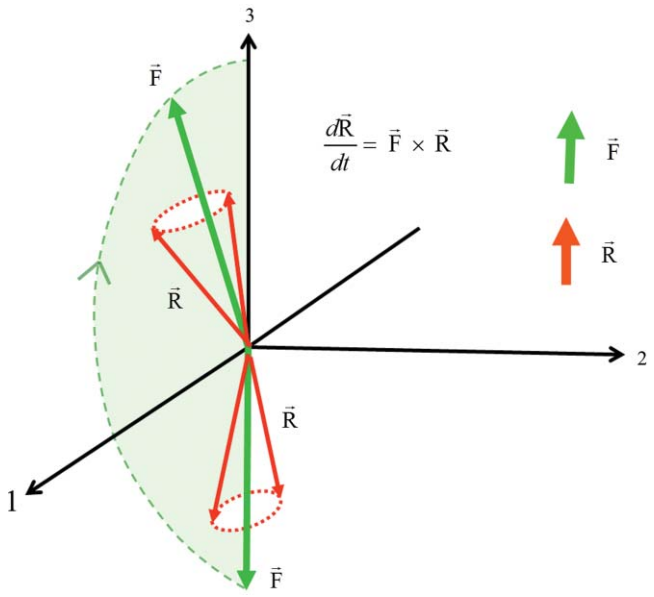

FIG. 1. Two-photon vector model for SARP. Motion of the two-photon Bloch vector $\vec{R}$ (red) $= [\mathrm{Re}(\sigma_{01}), \mathrm{Im}(\sigma_{01}), w]$ in the three-dimensional pseudo space adiabatically following the pseudo angular velocity vector $\vec{F}$ (green) $= [-2r, 0, -\delta_2]$. As the Raman detuning δ_2 reverses in the presence of overlapping pump and Stokes pulses shown in Fig. 2(c), the vector $\vec{F}$ swings from a $-\hat{z}$ to $+\hat{z}$ direction dragging along the strongly coupled Bloch vector $\vec{R}$. Reversal of $\vec{R}$ means population inversion between the Raman levels $v = 0$ and $v = 1$.

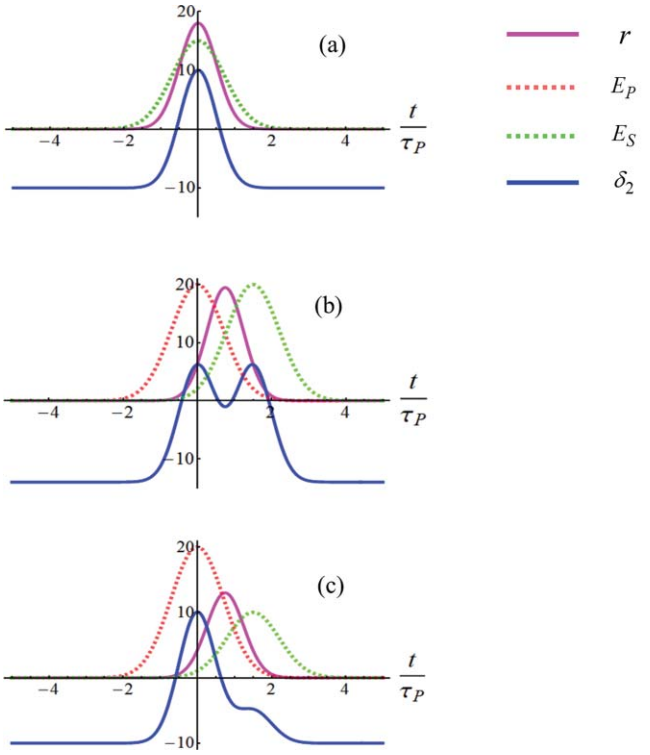

FIG. 2. Qualitative description of SARP using a sequence of overlapping pump and Stokes pulses of different relative delays and intensity ratios. Sweeping of the Raman detuning δ_2 (blue) is shown together with the Raman coupling r (magenta), pump optical field (red, dashed), Stokes optical field (green, dashed) in arbitrary units as a function of pulse time in units of pulse duration τ_P. (a) Zero-delay between pump and Stokes pulses generates two crossings for the detuning δ_2 (blue) in the region of maximum interaction that is large value of r (magenta). Only the Stokes field E_S (green, dashed) is shown for the identical and coincident pump and Stokes fields. (The two-photon Bloch vector flips twice during the Raman interaction, causing population transfer back and forth between $v = 0$ and $v = 1$ level, the case of CPR.) (b) Delayed pump and Stokes pulses of equal amplitude generates multiple zero-crossing of detuning δ_2 during the peak of Raman interaction r. Coherent population transfer and return occurs twice during the Raman interaction. (c) Two zero-crossings of δ_2 (blue) are generated using overlapping pump and Stokes pulses of a relative delay and an amplitude ratio. The first crossing appears in the beginning when r is negligible, and no population transfer takes place here. The second zero crossing appears near the peak of r (magenta) causing complete population inversion or flipping of the Bloch vector R as described in the text.

detuning can be expressed as

$$\delta_2 = \delta_0 - \delta_{AC} \cong \delta_0 + \frac{(\alpha_1 - \alpha_0)}{\hbar}[|E_P|^2 + |E_S|^2]. \quad (9)$$

Equation (9) implies that for a given zero-field detuning δ_0, a relative intensity and delay of the pump and Stokes pulses will be necessary to sweep δ_2 through zero near the central overlapping region where the Raman coupling $r \propto E_P E_S$ maximizes. We stress that population inversion or reversal of the Bloch vector $\vec{R}$ happens only when δ_2 crosses zero in the presence of appreciable two-photon coupling r between the pseudo vectors $\vec{F}$ and $\vec{R}$.

Figure 2 qualitatively describes the SARP idea by comparing the situations for three different pulse sequences: (a) zero delay, (b) delayed pulses with equal intensity, and (c) delayed pulses with unequal intensities. When the pulses are applied with zero delay, the detuning δ_2 crosses zero twice in the overlapping region where r is large (Figure 2(a)). During the Raman interaction, the Bloch vector flips twice, bringing the excited population back to the ground state. This situation is typical for coherent population return (CPR).[33] Figure 2(b) shows sweeping of δ_2 using delayed pump and Stokes pulses of equal intensities. The sequence generates multiple zero-crossing of δ_2 in the overlapping region, where r is appreciable again causing coherent population return to the ground state. Figure 2(c) shows the time-dependent detuning δ_2 in the presence of delayed pump and Stokes pulses of unequal intensities with the stronger pulse appearing first. In this example, δ_2 crosses zero twice. The first crossing appears in the beginning of the interaction, where r is negligible and no population transfer takes place here. The second crossing occurs near the peak of the Raman interaction in the central overlapping region where r is large, and most of the population transfer to the $v = 1$ excited level takes place during this time. The condition that r must be large near a single zero-crossing of δ_2 and negligible in all other crossings is just what is needed for SARP to invert population between the Raman allowed vibrational levels. We note that in DSCRAP (Ref. 24) the off-resonant Stark pulse controls the zero-crossings of the detunings associated with the near resonant pump and Stokes transitions between the metastable vibrational levels and the intermediate level in excited electronic state. We show here that it is possible to control the zero-crossing of the Raman detuning δ_2 without using an additional Stark pulse or an intermediate electronic level by appropriately overlapping the time-shifted pump and Stokes pulses of appropriate intensities. As δ_2 sweeps from a positive to a

negative value (Fig. 2(c)), the pseudo vectors $\vec{F}$ rotates from a negative to a positive direction relative to the $\hat{z}$ axis of the abstract space, dragging $\vec{R}$ along with it as discussed previously using Figure 1. Note that unlike STIRAP that has a resonant intermediate level,[8,9,19–21] the time ordering of the weak and strong pulses in SARP does not matter, and the flipping of the pseudo vector $\vec{R}$ can be accomplished with either sign of chirp $d\delta_2/dt$.

Although the optimal ratio of the intensities and delay that maximize the population transfer must be determined from a numerical analysis, a rough estimate of the required intensity ratio can be made. For example, the Stark shift of the Raman resonance $\delta_{AC} = \delta_1^{AC} - \delta_0^{AC}$ at the peak of the stronger pulse must be greater than $|\delta_0|$, which sets a threshold intensity for SARP. Using the Stark shift coefficients calculated for H_2 (see Table II in Sec. III), we estimate a peak intensity of ~15 GW/cm^2 for the stronger pulse that will generate an optimum Stark shift $\delta_{AC} \approx -1$ GHz to compensate for a zero-field detuning $\delta_0 = -0.5$ GHz. We can then sweep δ_2 appreciably ($\sim \pm 0.5$ GHz) in the overlapping region of the pump and Stokes pulses. In order to generate a steady sweep of δ_2 without crossing zero multiple times in the overlap region, the magnitude of the Stark shift δ_{AC} induced by the temporally displaced weaker pulse must be less than δ_0. Our detailed calculations show that the population transfer of H_2 molecules using SARP is optimized with a relative intensity ratio ≥ 4 and a delay $\sim 1.5\tau_P$ between the pump and Stokes Gaussian pulses of $1/e$ half-width τ_P.

III. H_2 $v = 0 \rightarrow v = 1$ TRANSITIONS USING SARP

There is much interest in using molecular hydrogen as a scattering target because of the simplicity of this molecule. As a specific application of SARP, we consider excitation of the $S(0)$ branch of Raman transition H_2 ($v = 0$, $J = 0$, $M = 0$) $\rightarrow$ ($v = 1$, $J = 2$, $M = 0$) using parallel ($\pi - \pi$) polarization of the Stokes (699 nm) and the pump (532 nm) laser pulses of duration ~7 ns with the pulse energy of ~12 mJ and 60 mJ. The specific choice of exciting the ground state H_2 ($v = 0$, $J = 0$, $M = 0$) with nuclear spin I = 0 eliminates the nuclear depolarization of the ($v = 1$, $J = 2$, $M = 0$) target state of para-hydrogen. The two-photon Rabi frequency r and the polarizabilities $\alpha(\omega)$ for $v = 0$ and $v = 1$ vibrational levels are calculated using Eqs. (3), (5) and (6). The M-dependent optical coefficients for connecting $0 \rightarrow k$ and $k \rightarrow 1$ transitions with $\Delta J = \pm 1$ selection rule are explicitly calculated for each parameter. In Eqs. (3)–(6), the vibronic part of μ_{ik} corresponds to the transition dipole moments $\langle v'|\mu|v = 0\rangle$ and $\langle v'|\mu|v = 1\rangle$ connecting the $v = 0$ and $v = 1$ vibrational levels of the ground electronic state with the vibrational level v' belonging to several different excited electronic states. The vibronic transition dipole moments are calculated using the vibrationally resolved transition probabilities of Ref. 34 for the vibronic bands $B^1\Sigma_u^+ - X^1\Sigma_g^+$, $C^1\Pi_u - X^1\Sigma_g^+$, and $B'^1\Sigma_u^+ - X^1\Sigma_g^+$. The calculated transition dipole moments (in Debye) for the 40 vibronic levels v' of the three excited electronic states are presented as a function of their transition frequencies in Table I. The calculated transition dipole moments include the Franck-Condon overlap factor $q^{v',v}$.[34,35] The two-photon Rabi frequency r and the dynamic Stark shifts for $v = 0 \rightarrow v = 1$ Raman transition are calculated using the transition dipole matrix elements of Table I for the pump and Stokes laser wavelength of 532 nm and 699 nm. These molecular parameters are expressed as follows:

$$r = \eta E_P E_S^*, \tag{10}$$

$$\delta_i^{AC} = -\left[\zeta_i^P |E_P|^2 + \zeta_i^S |E_S|^2\right], \tag{11}$$

where $i = 0$ or 1. The calculated coefficient η for the two-photon Rabi frequency r and Stark shift coefficients $\zeta_i^{P,S}$ are given in Table II. The Stark shift coefficients agree closely

TABLE I. Transition dipole moments $\langle v'|\mu|v\rangle$ used in the calculation of $v = 0 \rightarrow v = 1$ stimulated Raman pumping.

		$X^1\Sigma_g^+$ $v = 0$		$X^1\Sigma_g^+$ $v = 1$	
Transition	v'	$\varepsilon_{v'v}$(eV)	$\mu_{vv'}$(Debye)	$\varepsilon_{v'v}$(eV)	$\mu_{vv'}$(Debye)
$B^1\Sigma_u^+ - X^1\Sigma_g^+$	0	11.1750	0.1986	10.6590	0.5504
	1	11.3450	0.3544	10.8290	0.8499
	2	11.4950	0.5076	10.9790	0.9850
	3	11.6550	0.6215	11.1390	0.9639
	4	11.8050	0.6951	11.2890	0.8500
	5	11.9450	0.7336	11.4290	0.6712
	6	12.0950	0.7436	11.5790	0.4861
	7	12.2250	0.7318	11.7090	0.2760
	8	12.3250	0.6999	11.809	0.1219
	9	12.5250	0.6601	12.0090	0.0376
	10	12.6250	0.6285	12.1090	0.1553
	11	12.7250	0.5713	12.2090	0.2592
	12	12.8650	0.5359	12.3490	0.3121
	13	12.9850	0.4901	12.4690	0.3725
	14	13.0950	0.4366	12.5790	0.3919
	15	13.2050	0.3992	12.6890	0.4238
	16	13.3050	0.3603	12.7890	0.4188
	17	13.4050	0.3186	12.8890	0.4139
	18	13.5050	0.2948	12.9890	0.4092
	19	13.6050	0.2699	13.0890	0.3692
$C^1\Pi_u - X^1\Sigma_g^+$	0	12.2850	0.6963	11.7690	1.1781
	1	12.5750	0.8501	12.0590	0.7608
	2	12.8450	0.8234	12.3290	0.2212
	3	13.0950	0.7212	12.5790	0.1635
	4	13.3250	0.6015	12.8090	0.3814
	5	13.5550	0.4880	13.0390	0.4697
	6	13.7650	0.4051	13.2490	0.4864
	7	13.9450	0.3114	13.4290	0.4494
	8	14.1150	0.2467	13.5990	0.4125
	9	14.2750	0.1998	13.7590	0.3593
	10	14.4050	0.1567	13.8890	0.3096
	11	14.5250	0.1263	14.0090	0.2583
	12	14.6050	0.0991	14.0890	0.2091
	13	14.6750	0.0695	14.1590	0.1468
$B'^1\Sigma_u^+ - X^1\Sigma_g^+$	0	13.6950	0.2340	13.1790	0.4623
	1	13.9250	0.3297	13.4090	0.4560
	2	14.1250	0.3608	13.6090	0.3230
	3	14.3250	0.3533	13.8090	0.1737
	4	14.4950	0.3072	13.9790	0.0579
	5	14.6050	0.2344	14.0890	0.0061

TABLE II. The molecular parameters η, $\zeta_0^{P,S}$, and $\zeta_f^{P,S}$ for the two-photon Rabi frequency and Stark shifts for the $|0\rangle \rightarrow |f\rangle$ stimulated Raman transition. These parameters have been calculated using the transition dipole matrix elements of Table I.

Transition $\|vJM\rangle \rightarrow \|v'J'M'\rangle$	Pump wavelength λ_P(nm), polarization	Stokes wavelength λ_S(nm), polarization	$\eta \times 10^9$ rad/s/ (GW/cm^2)	$\zeta_0^{P,\pm} \times 10^9$ rad/s/ (GW/cm^2)	$\zeta_0^{S,\pm} \times 10^9$ rad/s/ (GW/cm^2)	$\zeta_f^{P,\pm} \times 10^9$ rad/s/ (GW/cm^2)	$\zeta_f^{S,\pm} \times 10^9$ rad/s/ (GW/cm^2)
$\|000\rangle \rightarrow \|120\rangle$	532, linear($\hat{z}$)	699, linear($\hat{z}$)	0.51	ζ_0^P 0.67	ζ_0^S 0.67	ζ_1^P 1.1	ζ_1^S 1.1
$\|000\rangle \rightarrow \|12 \pm 2\rangle$	532, circular ($\sigma^{\pm}$)	699, circular ($\sigma^{\mp}$)	−0.62	ζ_0^+ 0.67	ζ_0^- 0.67	ζ_1^+ 0.9	ζ_1^- 0.9
$\|000\rangle \rightarrow \|420\rangle$	355, linear($\hat{z}$)	795, linear($\hat{z}$)	0.61	ζ_0^P 0.67	ζ_0^S 0.67	ζ_4^P 1.77	ζ_4^S 1.63

with previous Raman calculations carried out for H_2 ($v = 1$, $J = 1$, M) by Dyer and Bischel[36] at somewhat different frequencies and branch transitions.

In Eqs. (10) and (11) the squares of the optical field amplitudes are normalized with respect to the optical intensity in GW/cm^2 using $E^2(\mathrm{V}^2/\mathrm{m}^2)/(\mathrm{GW/cm}^2) = 1.885 \times 10^{15}$. The density matrix equations (1) and (2) are numerically integrated using transform-limited single-mode laser pulses with electric fields that have the Gaussian shape $\sim\exp(-t^2/\tau_P^2)$ with $\tau_P = 6$ ns, the 1/e half-width of the Gaussian pulse. The single-mode phase coherent optical pulses are necessary to eliminate the phase fluctuations of the optical fields during the interaction time. In the presence of the delayed sequence of pump and Stokes laser pulses, the instantaneous two-photon Rabi frequency r and the dynamic Stark shifts are calculated using the ζ coefficients and the laser intensity profile at each step of time integration.

A. Almost complete population transfer in H_2 using SARP

Figure 3(a) shows complete population transfer to the H_2 ($v = 1$, $J = 2$, $M = 0$) level for a zero-field Raman detuning $\delta_0 = -0.4$ GHz when the pump and Stokes laser pulses are applied with a relative delay $\tau_D = 1.4\tau_P$. Optical fluences for the pump and Stokes pulses were assumed to be 557 mJ/mm^2 and 139 mJ/mm^2 corresponding to the amplitude ratio $E_P/E_S = 2$ for their optical fields. In Fig. 3(a) scaled Gaussian pulse profiles in arbitrary units (a.u.) are also plotted to show the interaction time in reference to the pulse centers. Figure 3(b) shows the dynamic Stark sweeping of the two-photon (Raman) detuning $\delta_2 = \delta_0 - \delta_{AC}$ in unit of GHz and the two-photon Rabi frequency r in arbitrary unit as a function of time. Figure 3(b) shows two zero-crossings of Raman detuning δ_2 (blue). The first crossing appears in the region of negligible r (magenta) and no population transfer takes place during this period as described previously in the context of Figure 2(c). Most of the population transfer takes place during the second crossing close to the peak of r (highlighted with a yellow circle in Fig. 3(b)). Figure 3(c) shows the components of the pseudo vectors $\vec{R}$ and $\vec{F}$ as a function of the interaction time. Figure 3(c) again shows that the zero-crossing of δ_2 in the presence of appreciable Raman coupling r allows the simultaneous reversal of the pseudo vectors $\vec{F}$ and $\vec{R}$ with respect to the $\hat{z}$ axis of the abstract space, thus inverting the population between the vibrational levels. Figure 3(d) provides a visual description of the Raman interaction (shown in Figs. 3(a)–3(c)) by giving the positions of the Bloch vector $\vec{R}$ (orange) which adiabatically follows the pseudo angular velocity vector $\vec{F}$ (green) in time for $t \geq -5$ ns, the starting point of the Raman interaction. In this example with a minimal two-photon coupling ($|F|^2 \approx d\delta_2/dt$), the Rabi oscillations (corresponding to the spinning of the Bloch vector $\vec{R}$ around $\vec{F}$) can be only seen near the end of the interaction.

Figure 4 compares the population transfer versus pump fluence for the case of zero delay (green) between the pump and Stokes pulses with that when the pulses are separated by $\tau_D = 1.4\tau_P = 8.4$ ns (red). The Stokes-to-pump field amplitude ratio of 2 and zero-field detuning $\delta_0 = -0.4$ GHz were kept the same for the two curves. Nearly complete population transfer to the $v = 1$ level is seen with the partially overlapping pulses. Small amplitude Rabi oscillations of the excited state population are seen for the case of zero delay. This is the case of CPR in the presence of a dynamic Stark shift. Figures 3 and 4 demonstrate what can be achieved with SARP under optimal conditions using currently available laser sources.

Figure 5 shows the fractional population transfer to the excited state H_2 ($v = 1$, $J = 2$, $M = 0$) as a function of the inter pulse delay for two different zero-field detunings $\delta_0 = -0.4$ GHz (dashed) and $\delta_0 = -0.5$ GHz (solid). With both zero-field detunings, over 90% population transfer can be achieved using SARP for the relative delay $\tau_D \approx \pm 1.5\tau_P$ between the Gaussian pump and Stokes pulses with the pulse lengths $\tau_P = \tau_S$. CPR occurs for the zero delay. Figure 5 shows that the population transfers do not depend upon the sign of the relative delay, i.e., the time ordering of the strong and weak pulses does not matter, which is expected because SARP works with both positive and negative chirps ($d\delta_2/dt$) of the Raman detuning δ_2. We note that the inter-pulse delay range for the complete population transfer becomes wider for a larger negative zero-field detuning $\delta_0 = -0.5$ GHz. A larger detuning, however, requires higher pump and Stokes laser intensities.

The optical intensity of the pump and Stokes pulses determines the two most important parameters, the dynamic Raman detuningδ_2 and the two-photon Rabi frequency r, which control the population transfer during the adiabatic Raman passage. Therefore, the population transfer by SARP needs to be optimized using the combined parameter space of the zero-field detuning δ_0 and optical pulse energy.

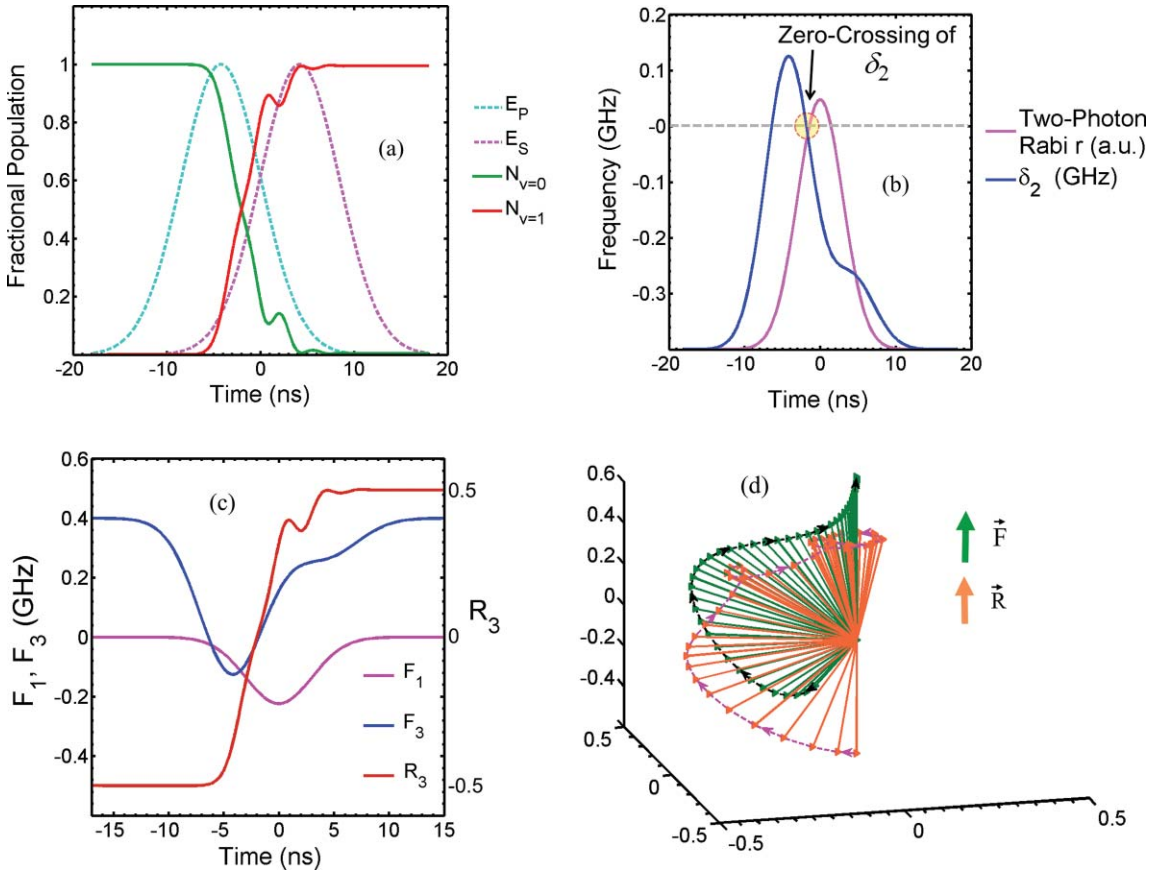

FIG. 3. SARP using delayed sequence of Gaussian pump and Stokes laser pulses with τ_P =6 ns, $\tau_D = 1.4\tau_P$ and fluences of 557 mJ/mm^2 and 139 mJ/mm^2, respectively. The field amplitude ratio of these energy densities is $E_P/E_S = 2$. Zero-field Raman detuning $\delta_0 = -0.4$ GHz. (a) Populations of the $H_2(v = 0,\ J = 0,\ M = 0)$ and $H_2(v = 1,\ J = 2,\ M = 0)$ state as functions of interaction time (green and red). (b) Time-dependent Raman detuning $\delta_2 = \delta_0 - (\delta_1^{AC} - \delta_0^{AC})$ (blue) and two-photon Rabi frequency r (a.u.) (magenta) as functions of time. (c) Components of pseudo vectors $\vec{F}$ and $\vec{R}$ as functions of time. (d) Adiabatic following of the Bloch vector $\vec{R}$ (red) around the pseudo angular velocity vector $\vec{F}$ (green) in the abstract space under the action of pump and Stokes laser pulses in time. The length of $\vec{F}$ has been scaled by a constant factor for better viewing. The pink arrows trace the time course.

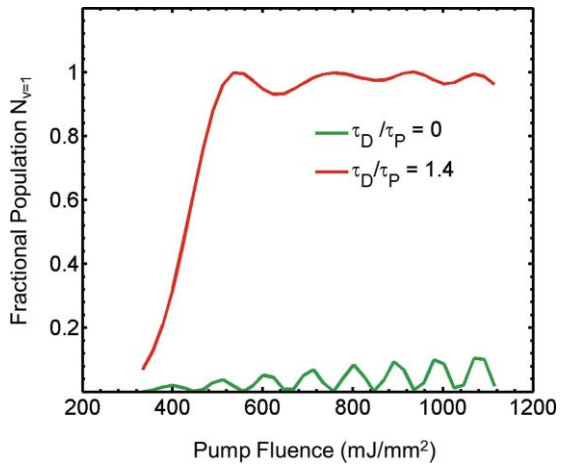

FIG. 4. Fractional population of the excited state ($v = 1,\ J = 2,\ M = 0$) versus pump pulse fluence for two inter-pulse delays: $\tau_D = 0$ (green) and $\tau_D = 1.4\tau_P$ (red). Pulse length $\tau_P = 6$ ns; zero-field detuning $\delta_0 = -0.4$ GHz; pump to Stokes optical field amplitude ratio $E_P/E_S = 2$. Near complete population transfer (red) is obtained using a delayed sequence of pump and Stokes pulses.

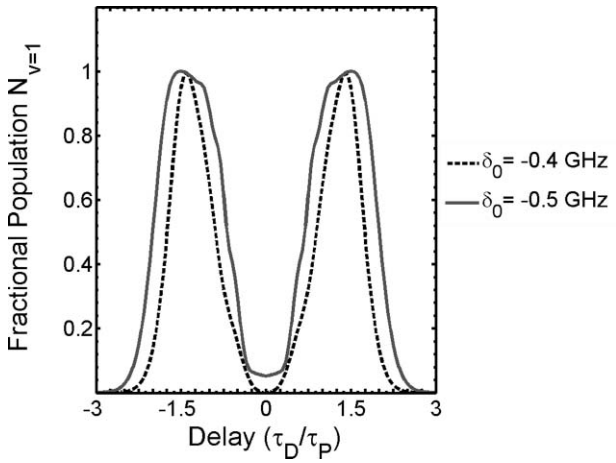

FIG. 5. Fractional population transferred to $H_2(v = 1,\ J = 2,\ M = 0)$ state versus delay between the pump and Stokes pulses for two zero-field detunings : $\delta_0 = -0.4$ GHz (dashed) and $\delta_0 = -0.5$ GHz (solid). Pulse length $\tau_P = \tau_S = 6$ ns. For $\delta_0 = -0.4$ GHz the pump and Stokes pulse fluences are 557 mJ/mm^2 and 139 mJ/mm^2, respectively, corresponding to their field amplitude ratio $E_P/E_S = 2$; For $\delta_0 = -0.5$ GHz the pump and Stokes pulses have fluences 1213 mJ/mm^2 and 250 mJ/mm^2 corresponding to $E_P/E_S = 2.2$.

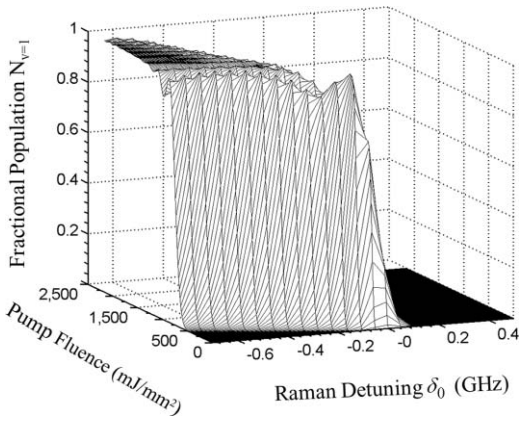

FIG. 6. Three-dimensional plot of the fractional population transfer to the $v = 1$ excited level as a function of pump pulse fluence (mJ/mm^2) and zero-field Raman detuning δ_0 (GHz) using SARP with delayed sequence of Gaussian pump and Stokes pulses with the temporal length $\tau_P = 6$ ns, inter-pulse delay $\tau_D = 1.4\tau_P$, and pump to Stokes field amplitude ratio $E_P/E_S = 2.2$.

Figure 6 shows a three-dimensional plot for the population transfer as a function of the pump fluence and the zero-field detuning δ_0. The pump-to-Stokes field amplitude ratio $E_P/E_S = 2.2$ was used for this computation. The graph shows that population transfer using SARP is achieved only with negative zero-field Raman detuning δ_0 because the dynamic Stark shifts of the rovibrational eigenstates $(v = 0,\ J = 0,\ M = 0)$ and $(v = 1,\ J = 2,\ M = 0)$ cause a net redshift for the $v = 0 \rightarrow v = 1$ transition. In this case, for a negative zero-field detuning $\delta_0 = \omega_P - \omega_S - \omega_{10}$, the dynamic Stark shift will sweep the net Raman detuning $\delta_2 = \delta_0 - (\delta_1^{AC} - \delta_0^{AC})$ through the zero value, which is necessary for transferring population via SARP. With larger detunings, the adiabatic transfer becomes more efficient.

Figure 7(a) provides a two-dimensional plot of the population transfer versus pump fluence for a set of discrete zero-field detunings δ_0 derived from Fig. 6. Figure 7(a) shows that SARP achieves complete population transfer with a threshold fluence which increases with the zero-field detuning δ_0. This behavior is expected because SARP requires the Stark shift of the Raman resonance $|\delta_{AC}| > |\delta_0|$ [see Eq. (9)]. Beyond a certain energy, the population transfer decreases with pulse energy for a given δ_0. This is because at a large fluence the dynamic Stark shift overcompensates the zero-field detuning, which according to Eq. (9) prevents δ_2 from crossing zero not until very late when r has significantly fallen as is the case for $\delta_0 = -0.3$ GHz (Figure 7(b)). Figure 7(b) demonstrates that for the same pulse fluence with $\delta_0 = -0.5$ GHz, zero-crossing of δ_2 near the peak of r enables complete population transfer to $v = 1$ level.

Figure 8 is a two-dimensional contour plot showing the range of the pump fluence that will allow greater than 90% population transfer as a function of the zero-field detunings δ_0 corresponding to the three-dimensional plot of Figure 6. With larger $|\delta_0|$, a wider range of pulse fluences is able to achieve nearly complete population transfer to $v = 1$ vibrational level (Figure 8). Larger $|\delta_0|$, however, requires higher threshold

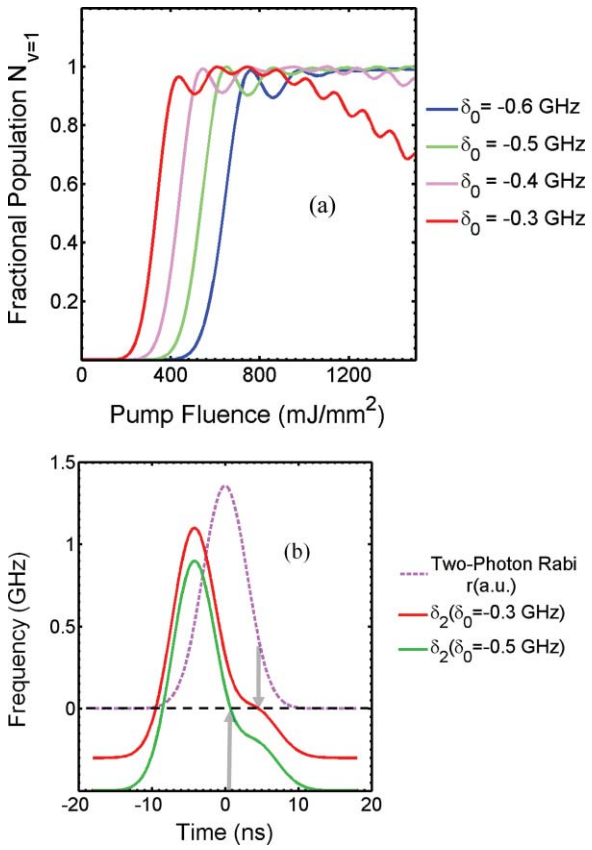

FIG. 7. (a) Population transfer versus pump pulse fluence (mJ/mm^2) for the zero-field detunings $\delta_0 = -0.3,\ -0.4,\ -0.5,\ -0.6$ GHz. The pump and Stokes pulse sequence is the same as in Fig. 6. (b) For the pump pulse fluence of ~1500 mJ/mm^2, the time evolution of the Stark shifted detuning δ_2 is compared for the two zero-field detunings $\delta_0 = -0.3$ GHz (red) and $\delta_0 = -0.5$ GHz (green). The pump fluence corresponds to a peak intensity of ~20 GW/cm^2. The relative delay and amplitude ratio of the pulse sequence are the same as in (a).

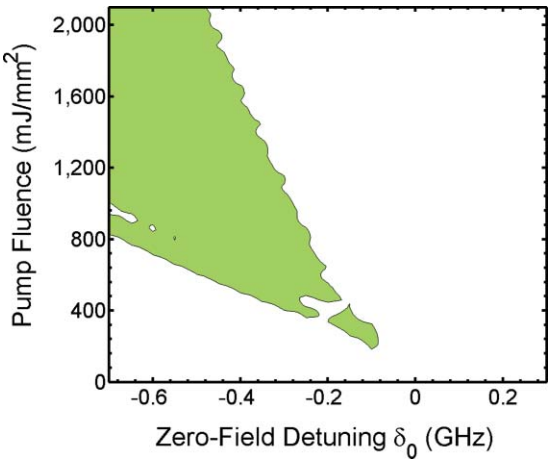

FIG. 8. Contour map showing the pump pulse fluence (mJ/mm^2) as a function of the zero-field detuning δ_0 (GHz) that can achieve greater than 90% population transfer to $v = 1$ level using SARP with the delayed sequence of pump and Stokes laser pulses. All other pulse parameters are the same as in Fig. 6.

fluence, as shown in Figures 6 and 7. To reduce other nonlinear (hyper-Raman) optical processes, we limit the peak intensity of the stronger pulse to less than 20 GW/cm^2 which corresponds to a fluence ~1500 mJ/mm^2 for the Gaussian pulse with $\tau_p = 6$ ns.

Based upon these data, we suggest that significant population transfer (in excess of 90%) can be obtained using Stokes and pump pulses with duration ~7 ns (FWHM of intensity) and energy 12 mJ and 60 mJ focused within a beam of diameter 0.25 mm. Because the phase coherence of the optical pulses is essential, SARP requires single-mode, transform-limited optical pulses. Frequency-doubled injection-seeded single-mode Nd^{3+}:YAG laser pulses at 532 nm with coherence length 8–10 ns are commercially available and provides a good source for the pump. A narrow linewidth single-mode Stokes laser pulse may be prepared by seeding a cw single mode laser at 699 nm to a three-stage dye amplifier pumped by the 532-nm Nd^{3+}:YAG laser as demonstrated by Drell *et al.*[37] In this way, transform-limited Stokes pulses of energy ~12 mJ can be generated with the same pulse duration as the pump laser at 532 nm.

Molecules pumped into the excited state ($v = 1$, $J = 2$, $M = 0$) will have their $\boldsymbol{J}$ vectors strongly polarized in a plane perpendicular to the $\hat{z}$ axis. We note that using SARP with a left circularly polarized $\sigma^+ = -(\hat{x} + i\hat{y})/\sqrt{2}$ pump and a right circularly polarized $\sigma^- = (\hat{x} - i\hat{y})/\sqrt{2}$ Stokes wave result in a population of ($v = 0$, $J = 0$, $M = 0$) state transferred to the ($v = 1$, $J = 2$, $M = 2$) state. It creates an ensemble of vibrationally excited molecules with their $\boldsymbol{J}$ vectors oriented along the $+\hat{z}$ direction. Similarly, the complete population transfer to ($v = 1$, $J = 2$, $M = -2$) and $\boldsymbol{J}$-polarization along the $-\hat{z}$ axis can be achieved using the $\sigma^- - \sigma^+$ SARP. For the circular polarization the quantization axis $\hat{z}$ refers to the propagation direction of the optical beams. The M-dependent two-photon Rabi frequency r and Stark shift parameters for the ($v = 0$, $J = 0$, $M = 0$) → ($v = 1$, $J = 2$, $M = 2$) Raman transition with σ^+ and σ^- pump and Stokes waves are defined as follows:

$$r = \eta E_P^+ E_S^{-*}, \tag{12a}$$

$$\delta_i^{AC} = -\left[\zeta_i^+ |E_P^+|^2 + \zeta_i^- |E_S^-|^2\right], \tag{12b}$$

where E_P^+ and E_S^- are the slowly varying envelopes of the σ^+ pump and σ^- Stokes waves respectively. $i = 0, 1$ correspond to the eigenstates ($v = 0$, $J = 0$, $M = 0$) and ($v = 1$, $J = 2$, $M = 2$). The molecular parameters η, $\zeta_0^{\pm}$, and $\zeta_1^{\pm}$ are given in Table II.

The value of the Stark shift coefficients for the ground ($v = 0$) and excited ($v = 1$) states suggest that compared to the $\pi - \pi$ Raman transition [see Table II], the $\sigma^+ - \sigma^-$ Raman transition will require a higher laser intensity to cause a comparable Stark shift of the Raman resonance. Our calculations show that for a zero-field detuning $\delta_2 = -0.3$ GHz, nearly complete population transfer to the excited state $H_2(v = 1, J = 2, M = 2)$ will be achieved using the optical fluence 947 mJ/mm^2 and 237 mJ/mm^2 for the pump and Stokes pulses. The optical fluence of the stronger pulse corresponds to the peak intensity ~13 GW/cm^2. With a larger zero-field detuning $\delta_0 < -0.3$ GHz, a peak intensity >20 GW/cm^2 will be required.

IV. H_2 $v = 0 \rightarrow v = 4$ TRANSITIONS USING SARP

A fixed wavelength pump laser at 355 nm (third harmonic Nd:YAG^{3+} at 1.06 μm) and a tunable Stokes laser pulse near ~795 nm (derived from 532-nm Nd:YAG^{3+} pumped parametric oscillator) may be used for pumping the $S(0)$ branch of H_2 $v = 0 \rightarrow v = 4$ Raman transition. The coefficients for the Stark shift and two-photon Rabi frequency for the $S(0)$ H_2 $v = 0 \rightarrow v = 4$ transition with the $\hat{z}$ polarized parallel pump and Stokes waves are calculated following the same procedures described in Sec. III and are given in Table II.

Here SARP benefits from the advantage of a large molecular polarizability of $v = 4$ level which gives rise to a substantial AC Stark shift of the Raman resonance. With an appreciable two-photon Rabi frequency coefficient η and the substantially different Stark shift coefficients $\zeta_4^{P,S}$ and $\zeta_0^{P,S}$ for the two vibrational levels as given in Table II, SARP can be achieved with a wide range of detunings and intensities as discussed using results of numerical analysis for H_2 $v = 0 \rightarrow v = 4$ transition. Gaussian pump and Stokes pulses with a relative delay $\tau_D = 1.5\tau_P$ and an optical field amplitude ratio 2.2 has been assumed for the calculation.

Figure 9 shows the population transfer to $v = 4$ level as a function of pump fluence for the various zero-field detunings δ_0. For each zero-field detuning, there is a threshold fluence to achieve complete population transfer to $v = 4$ level. As in the case of $v = 0 \rightarrow v = 1$ transition, the threshold fluence increases with the zero-field detuning because the adiabatic inversion of the Bloch vector requires $|\delta_{40}^{AC}| > |\delta_0|$. Figure 9 shows that for a given zero-field detuning, there is a range of pulse fluences for which the complete population transfer takes place. At higher fluence, the population transfer is reduced. This is because at higher fluences, $|\delta_{40}^{AC}|$ over-compensates the zero-field detuning and prevents δ_2 from crossing zero during the peak of Raman interaction (Figure 7(b)).

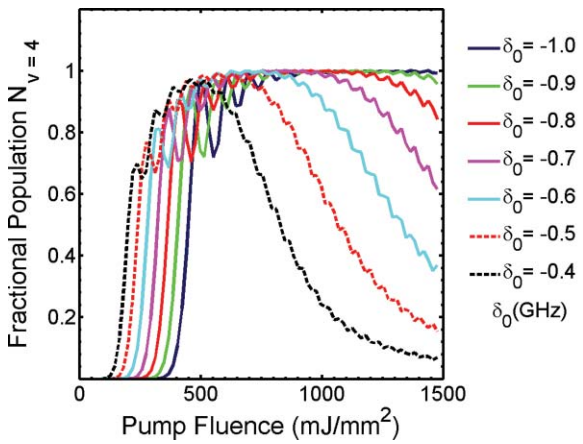

FIG. 9. Population transfer from the $v = 0$ ground to $v = 4$ excited vibrational level as a function of pump fluence (mJ/mm^2) for various detunings δ_0 in GHz. The calculations assume a UV pump pulse at 355 nm and a Stokes pulse near 795 nm with a relative field amplitude ratio of 2.2 and delay $\tau_D = 1.5\tau_P$.

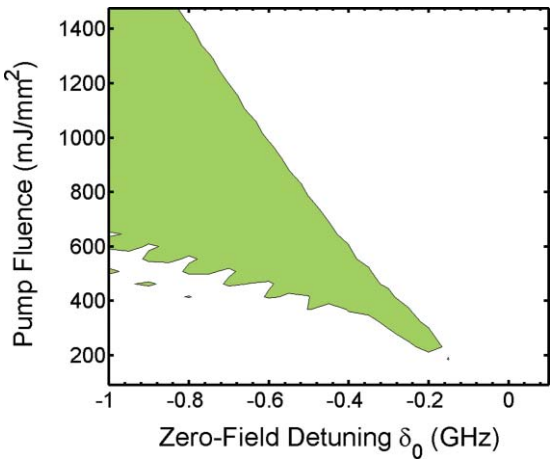

FIG. 10. Contour map showing the range of pump fluence (mJ/mm^2) and detuning δ_0 (GHz) that can achieve greater than 90% population transfer from the $v = 0$ ground to $v = 4$ excited vibrational level. The pulse sequence is the same as in Fig. 9.

The contour map of Fig. 10 shows the range of pump pulse (355 nm) fluences as a function of the zero-field detuning that achieves greater than 90% population transfer from $v = 0$ to $v = 4$. In the presence of a net negative AC Stark shift of the Raman resonance frequency ω_{40}, population transfer is achieved only for the negative detuning $\delta_0 = \omega_P - \omega_S - \omega_{40}$. Figure 10 shows that with larger zero-field detuning $|\delta_0| \geq 0.5$ GHz and pulse fluence >500 mJ/mm^2, complete population transfer becomes feasible over a broader range of pulse fluence and detuning. These fluences may be reached using a standard injection-seeded Nd^{3+}:YAG laser system.

V. CONCLUSION

We have shown that the dynamic Stark shifts of the Raman resonance generally limit the efficiency of stimulated Raman pumping when excited by transform-limited pump and Stokes pulses with zero delay. Increasing the intensity of the pulses does not promote the coherent population transfer. The Stark shift of the rovibrational levels grows with the laser intensity and throws the system off resonance, causing coherent return of the transiently excited population. However, this dynamic Stark shift can be manipulated to achieve the complete population inversion between two vibrational levels of the electronic ground state of a molecule. This goal is achieved using SARP with partially overlapping pump and Stokes pulses with a relative delay ($\sim 1.5\tau_P$) and intensity ratio (≥ 4). This method requires single-mode, transform-limited laser pulses of nanosecond duration. Preparation of vibrationally excited molecular target using SARP is not limited to $\Delta v = 1$. To support the last statement our theoretical analysis was extended to show complete population transfer from $H_2(v = 0,\ J = 0,\ M = 0)$ to H_2 $(v = 4, J = 2, M = 0)$ using standard laser sources with peak intensity less than 20 GW/cm^2.

ACKNOWLEDGMENTS

We thank Dudley Herschbach, Stephen E. Harris, Steven Stolte, James Parker, and Klaas Bergmann for critically reading the manuscript and for their helpful suggestions. This work has been supported by the U.S. Army Research Office (ARO) under ARO grant W911NF-10-1-01318.

[1] R. N. Zare, Science **279**, 1875 (1998).
[2] F. F. Crim, Proc. Natl. Acad. Sci. U.S.A. **105**, 12654 (2008).
[3] R. D. Beck, P. Maroni, D. C. Papageorgopoulos, T. T. Dang, M. P. Schmid, and T. R. Rizzo, Science **302**, 98 (2003).
[4] J. C. Tully, Science **312**, 1004 (2006).
[5] A. J. Orr-Ewing and R. N. Zare, Annu. Rev. Phys. Chem. **45**, 315 (1994).
[6] A. J. Alexander, M. Brouard, K. S. Kalogerakis, and J. P. Simons, Chem. Soc. Rev. **27**, 405 (1998).
[7] *Vector Correlation and Alignment in Chemistry*, edited by Gabriel G. Balint-Kurti and Marcelo P. de Miranda (CCP6, Warrington, UK, 2006).
[8] N. Mukherjee and R. N. Zare, J. Chem. Phys. **131**, 164302 (2009).
[9] N. Mukherjee and R. N. Zare, J. Chem. Phys. **132**, 154302 (2010).
[10] R. L. Farrow and D. W. Chandler, J Chem. Phys. **89**, 1994 (1988).
[11] G. O. Sitz and R. L. Farrow, J Chem. Phys. **101**, 4682 (1994).
[12] N. C. M. Bartlett, D. J. Miller, R. N. Zare, D. Sofikitis, T. P. Rakitzis, and A. J. Alexander, J. Chem. Phys. **129**, 084312 (2008).
[13] S. A. Kandel, A. J. Alexander, Z. H. Kim, R. N. Zare, F. J. Aoiz, L. Bañares, J. F. Castillo, and V. Sáez Rábanos, J. Chem. Phys. **112**, 670 (2000).
[14] D. Grischkowski and M. M. T. Loy, Phys. Rev. A **12**, 1117 (1975).
[15] D. Grischkowski, M. M. T. Loy, and P. F. Liao, Phys. Rev. A **12**, 2514 (1975).
[16] M. M. T. Loy and D. Grischkowski, Opt. Commun. **21**, 379 (1977).
[17] M. M. T. Loy, Phys. Rev. Lett. **41**, 473 (1978).
[18] A. D. Rudert, J. Martin, H. Zacharias, and J. B. Halpern, Chem. Phys. Lett. **294**, 381 (1998).
[19] N. V. Vitanov, M. Fleischhauer, B. W. Shore, and K. Bergmann, Adv. At., Mol., Opt. Phys. **46**, 55 (2001).
[20] K. Bergmann, H. Theuer, and B. W. Shore, Rev. Mod. Phys. **70**, 1003 (1998), and references therein.
[21] U. Gaubatz, P. Rudeck, S. Schiemann, and K. Bergmann, J. Chem. Phys. **92**, 5363 (1990).
[22] T. Rickes, L. P. Yatsenko, S. Steuerwald, T. Halfmann, B. W. Shore, and N. V. Vitanov, and K. Bergmann, J. Chem. Phys. **113**, 534 (2000).
[23] L. P. Yatsenko, N. V. Vitanov, B. W. Shore, T. Rickes, and K. Bergmann, Opt. Commun. **204**, 413 (2002).
[24] M. Oberst, H. Muench, G. Grigoryan, and T. Halfmann, Phys. Rev. A **78**, 033409 (2008).
[25] S. Chelkowski and A. D. Bandrauk, J. Raman Spectrosc. **28**, 459 (1997).
[26] F. Legare, S. Chelkowski, and A. D. Bandrauk, Chem. Phys. Lett. **329**, 469 (2000).
[27] L. P. Yatsenko, S. Guerin, and H. R. Jauslin, Phys. Rev. A **65**, 043407 (2002).
[28] N. Mukherjee, J. Opt. Soc. Am. B **23**, 1635 (2006).
[29] J. F. Ward, Rev. Mod. Phys. **37**, 118 (1965); P. W. Milonni, and J. H. Eberly, J. Chem. Phys. **68**, 16021613 (1978); B. W. Shore and R. J. Cook, Phys. Rev. A **20**, 1958 (1979); B. W. Shore, Phys. Rev. A **34**, 1413 (1981); B. W. Shore, *The Theory of Coherent Atomic Excitation* (Wiley, New York, 1990), Sec. 14.8; N. V. Vitanov and S. Stenholm, Phys. Rev. A **55**, 648 (1997).
[30] L. Allen and J. H. Eberly, *Optical Resonance and Two level Atoms* (Wiley, New York, 1975).
[31] J. P. Marangos, J. Mod. Opt. **45**, 471 (1998).
[32] R. L. Shoemaker, Annu. Rev. Phys. Chem. **30**, 239 (1979).
[33] N. Vitanov, B. Shore, L. Yatsenko, K. Boehmer, T. Halfmann, T. Rickes, and K. Bergmann, Opt. Commun. **199**, 117 (2001).
[34] U. Fantz and D. Wuennderlich, At. Data Nucl. Data Tables **92**, 853 (2006).
[35] M. Larsson, Astron. Astrophys. **128**, 291 (1983).
[36] M. J. Dyer and W. K. Bischel, Phys. Rev. A **44**, 3138 (1991).
[37] P. Drell and S. Chu, Opt. Commun. **28**, 343 (1979).